Cell Reports



# Vesicular Glutamate Transporter Expression Ensures High-Fidelity Synaptic Transmission at the Calyx of Held Synapses

## Graphical Abstract

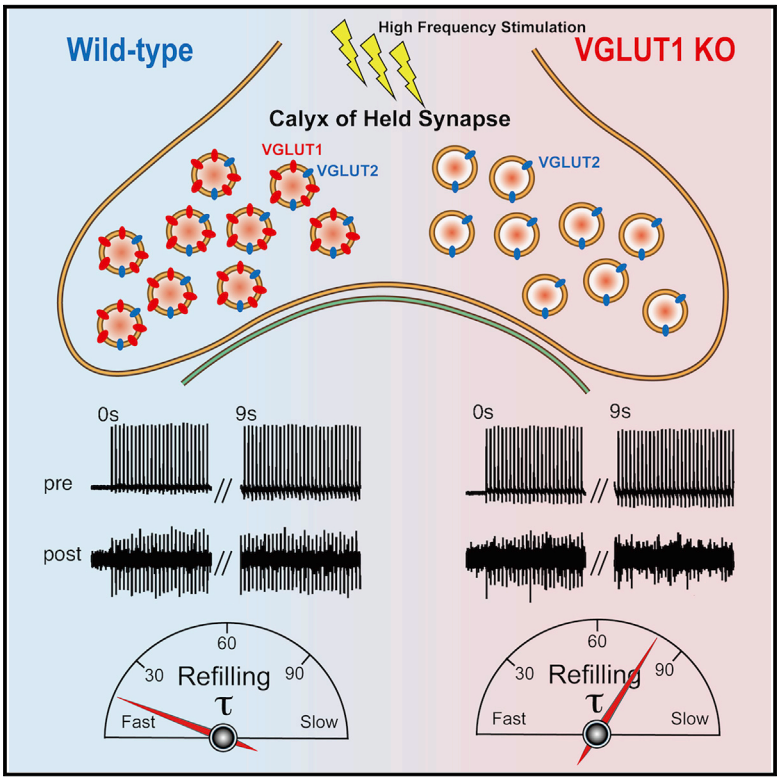


## Highlights

- Basal synaptic transmission in VGLUT1-KO calyx of Held synapses is largely intact
- VGLUT1 loss slows down SV refilling with glutamate
- VGLUT1 loss leads to abnormal synaptic failures during sustained stimulation
- The speed of glutamate loading into SVs can be rate limiting for neurotransmission

## Authors

Yutaro Nakakubo, Saeka Abe, Tomofumi Yoshida, ..., Nils Brose, Shigeo Takamori, Tetsuya Hori

## Correspondence

stakamor@mail.doshisha.ac.jp (S.T.), tetsuya.hori@oist.jp (T.H.)

## In Brief

Glutamate loading into synaptic vesicles (SVs) is indispensable for excitatory neurotransmission. Yet it is unclear whether the speed of glutamate loading is rate limiting. Here, Nakakubo et al. report that glutamate loading is slowed down in VGLUT1-KO calyx of Held synapses, which consequently results in abnormal synaptic failures during sustained stimulation.

Nakakubo et al., 2020, Cell Reports *32*, 108040
August 18, 2020 © 2020 The Author(s).
https://doi.org/10.1016/j.celrep.2020.108040

CellPress

Cell Reports

CellPress
OPEN ACCESS

Report

# Vesicular Glutamate Transporter Expression Ensures High-Fidelity Synaptic Transmission at the Calyx of Held Synapses

Yutaro Nakakubo,[1,5] Saeka Abe,[1,5] Tomofumi Yoshida,[2,5] Chihiro Takami,[2] Masayuki Isa,[2] Sonja M. Wojcik,[3] Nils Brose,[3] Shigeo Takamori,[2,*] and Tetsuya Hori[1,4,6,*]

[1]Department of Neurophysiology, Graduate School of Life and Medical Sciences, Doshisha University, Kyoto 610-0394, Japan
[2]Laboratory of Neural Membrane Biology, Graduate School of Brain Science, Doshisha University, Kyoto 610-0394, Japan
[3]Department of Molecular Neurobiology, Max Planck Institute for Experimental Medicine, Göttingen 37075, Germany
[4]Present address: Cellular and Molecular Synaptic Function Unit, Okinawa Institute of Science and Technology Graduate University, Okinawa 904-0495, Japan
[5]These authors contributed equally
[6]Lead Contact
*Correspondence: stakamor@mail.doshisha.ac.jp (S.T.), tetsuya.hori@oist.jp (T.H.)
https://doi.org/10.1016/j.celrep.2020.108040

## SUMMARY

Recycling of synaptic vesicles (SVs) at presynaptic terminals is required for sustained neurotransmitter release. Although SV endocytosis is a rate-limiting step for synaptic transmission, it is unclear whether the rate of the subsequent SV refilling with neurotransmitter also influences synaptic transmission. By analyzing vesicular glutamate transporter 1 (VGLUT1)-deficient calyx of Held synapses, in which both VGLUT1 and VGLUT2 are co-expressed in wild-type situation, we found that VGLUT1 loss causes a drastic reduction in SV refilling rate down to ~25% of wild-type values, with only subtle changes in basic synaptic parameters. Strikingly, VGLUT1-deficient synapses exhibited abnormal synaptic failures within a few seconds during high-frequency repetitive firing, which was recapitulated by manipulating presynaptic $Cl^-$ concentrations to retard SV refilling. Our data show that the speed of SV refilling can be rate limiting for synaptic transmission under certain conditions that entail reduced VGLUT levels during development as well as various neuropathological processes.

## INTRODUCTION

At chemical synapses, neurotransmitters are released from synaptic vesicles (SVs) by exocytosis. SVs are then regenerated by endocytosis and refilled with neurotransmitter to contribute to subsequent rounds of exocytosis (Südhof, 2004). Although endocytosis is a rate-limiting step for the maintenance of synaptic transmission at many synapses (e.g., Yamashita et al., 2005), it has so far not been investigated whether the speed of neurotransmitter refilling of SVs contributes to synaptic efficacy. In principle, SV refilling cannot be rate limiting for synaptic transmission unless the time it requires exceeds the time needed for SV reuse. However, some evidence has emerged to indicate very rapid endocytosis and SV reuse (Chung et al., 2010; Delvendahl et al., 2016; Ertunc et al., 2007; Ikeda and Bekkers, 2009; Watanabe et al., 2013, 2014), which may operate at shorter timescales than SV refilling, with time constants of ~15 s for glutamate (Hori and Takahashi, 2012) and ~20–50 s for GABA (Egashira et al., 2016; Yamashita et al., 2018). On the basis of these data, it is possible that the SV refilling process limits synaptic efficacy under certain conditions (e.g., during repetitive stimulation).

Glutamate is the major excitatory neurotransmitter in the mammalian central nervous system, and three vesicular glutamate transporters (VGLUT1–3) are responsible for the refilling of glutamate into SVs (Takamori, 2006). All VGLUTs use a proton electrochemical gradient generated by the vacuolar-type $H^+$ ATPase (V-ATPase) and exhibit similar transport kinetics and dependencies on surrounding ions, in particular $Cl^-$ (Edwards, 2007; Kaneko and Fujiyama, 2002). The most striking difference between the three VGLUTs is their distribution in the brain. Essentially, two major VGLUTs, VGLUT1 and VGLUT2, are expressed in a complementary fashion in the adult brain (Fremeau et al., 2001; Fujiyama et al., 2001): VGLUT1 is expressed mainly in cerebral cortex and hippocampus, whereas VGLUT2 is expressed in thalamus and brainstem. The minor isoform VGLUT3 is expressed only in subpopulations of neurons (e.g., in hippocampus), many of which are known to release other neurotransmitters, such as GABA and acetylcholine (Fremeau et al., 2002; Gras et al., 2002). Consistent with their complementary expression patterns, the deletion of different VGLUTs in mice causes a dramatic impairment of glutamatergic transmission in the respective brain areas (Fremeau et al., 2004; Weston et al., 2011; Wojcik et al., 2004). Interestingly, the expression levels of VGLUTs were shown


This is an open access article under the CC BY license (http://creativecommons.org/licenses/by/4.0/).

to define the steady-state glutamate content of SVs, although contradictory results were reported regarding the effect of reduced VGLUT expression (Daniels et al., 2004, 2006; Fremeau et al., 2004; Moechars et al., 2006; Weston et al., 2011; Wilson et al., 2005; Wojcik et al., 2004). However, the important issue as to whether VGLUT expression levels can regulate the speed of vesicle refilling and thereby affect synaptic efficacy and endurance has never been addressed.

To study the synaptic effects of the differential expression of VGLUT isoforms and of overall VGLUT expression levels, we compared glutamatergic synaptic transmission between wild-type and *VGLUT1*$^{-/-}$ mice using the calyx of Held as a model synapse. This synapse is glutamatergic and normally contains both VGLUT1 and VGLUT2 (Billups, 2005; Blaesse et al., 2005), and unlike other preparations of VGLUT-deficient animals examined so far, the large size of its presynaptic terminal allows combined pre- and postsynaptic patch-clamp recordings so that SV refilling can be studied by a combination of presynaptic washout and subsequent photolysis of caged glutamate (Hori and Takahashi, 2012). Our study demonstrates that deletion of VGLUT1 in calyx of Held synapses causes only subtle alterations in basic synaptic parameters, such as short-term plasticity, but leads to a defined decrease of the rate of glutamate refilling into SVs to ~25% compared with wild-type values. Accordingly, synaptic responses of VGLUT1-deficient synapses during high-frequency stimulation showed abnormal synaptic failures, indicating that the speed of neurotransmitter refilling of SVs can be rate limiting for synaptic transmission under certain physiological or pathophysiological conditions.

## RESULTS

### Normal Miniature and Evoked EPSCs in VGLUT1-Deficient Calyx of Held Synapses

Hippocampal synapses of *VGLUT1*$^{-/-}$ mice show markedly reduced evoked excitatory postsynaptic currents (EPSCs) because VGLUT1 is the dominant VGLUT isoform in these synapses (Fremeau et al., 2004; Weston et al., 2011; Wojcik et al., 2004). In contrast, calyx of Held synapses express both VGLUT1 and VGLUT2 (Billups, 2005; Blaesse et al., 2005). We therefore first tested whether deletion of VGLUT1 would alter expression of VGLUT2 at this synapse. To this end, immunolabeling experiments using antibodies specific for VGLUT1, VGLUT2, and VGLUT3 were performed in wild-type and *VGLUT1*$^{-/-}$ brainstem slices at the age of postnatal day 19 (P19) (Figures 1A and S1). As a control for the distribution of SVs, an anti-synaptophysin (Syp) antibody was used. Consistent with earlier reports (Billups, 2005; Blaesse et al., 2005), we observed similar patterns of VGLUT1 and VGLUT2 immunoreactivities, indicative of the calyx-type giant presynaptic terminals surrounding the MNTB principal neuron cell bodies, which overlapped with the majority of Syp-positive presynaptic structures in wild-type preparations (Figure 1A, upper panels). Although merged images clearly showed substantial populations of vesicle clusters that were dominated by one of the two VGLUT isoforms, line-scan analyses of several different portions of the presynaptic terminals demonstrated that each vesicle cluster that was double positive for Syp and one of the two VGLUT isoforms contained detectable levels of the respective other VGLUT isoform (Figure S1A). In contrast, VGLUT3 immunoreactivity was not observed within the calyx of Held terminals but instead appeared as grainy and diffusively sparse signals over the cell bodies of the MNTB principal neurons (Figure S1B). In *VGLUT1*$^{-/-}$ brainstem slices, we observed no VGLUT1 staining, confirming the genetic deletion (Figure 1A, lower panels). VGLUT2 staining did not differ between wild-type and *VGLUT1*$^{-/-}$ preparations. Although the VGLUT3 signal appeared slightly increased in *VGLUT1*$^{-/-}$ samples, this staining was clearly not synaptic (Figure S1B), indicating that VGLUT2 and VGLUT3 are not substantially upregulated to compensate for the loss of VGLUT1 in calyx of Held terminals.

To characterize the effects of VGLUT1 loss, we first recorded evoked EPSCs (eEPSCs) induced by single-fiber stimulation of afferent axon bundles. We observed no significant differences in eEPSC amplitudes between wild-type and *VGLUT1*$^{-/-}$ synapses (Figures 1B and 1C). Likewise, the amplitude and frequency of miniature EPSCs (mEPSCs) were not altered in *VGLUT1*$^{-/-}$ synapses compared with wild-type (Figures 1D–1G), indicating that VGLUT1 is dispensable and that VGLUT2 expression is sufficient to maintain normal quantal size and quantal content in calyx of Held synapses, at least under conditions of low-intensity stimulation. We also confirmed that VGLUT1 loss did not cause an upregulation of postsynaptic sensitivity (Figures S1C–S1E). Additionally, the unchanged mEPSC frequency and amplitudes seen in VGLUT1-deficient preparations indicate that VGLUT1 and VGLUT2 are likely present on the same SVs in the wild-type situation. This conclusion is in accordance with an older study we conducted, showing that VGLUT1 and VGLUT2 are co-localized in at least a subpopulation of SVs (Herzog et al., 2006), but contradicts an alternative view, according to which VGLUT1 and VGLUT2 segregate to different transmitter release sites in hippocampal neurons (Fremeau et al., 2004). The latter scenario would be compatible with our present findings only if VGLUT1 were a very minor VGLUT isoform in calyx of Held synapses, but this does not seem to be the case (see below).

### Slightly Perturbed Short-Term Plasticity and Recovery from Depression in VGLUT1-Deficient Calyx of Held Synapses

Previous studies using hippocampal preparations derived from *VGLUT1*$^{-/-}$ mice revealed that synapses lacking VGLUT1 have distinct properties. For instance, the remaining synaptic responses in *VGLUT1*$^{-/-}$ indicate higher release probability than seen in wild-type synapses, and the recovery from synaptic depression after repetitive stimulation is slower in VGLUT1-deficient synapses compared with their wild-type counterparts (Fremeau et al., 2004; Herman et al., 2014; Weston et al., 2011; Wojcik et al., 2004). On the basis of the fact that at least some hippocampal neurons also express VGLUT2, these distinct features seen in VGLUT1-deficient synapses have typically been attributed to the presence of VGLUT2 (Fremeau et al., 2004; Herman et al., 2014; Weston et al., 2011; Wojcik et al., 2004), although it is possible that other components of the respective synapses are at the core of these different features. Given that calyx of Held synapses normally express VGLUT1 and VGLUT2 on the same vesicles (Figures 1D–1G), we addressed the issue of functional differences

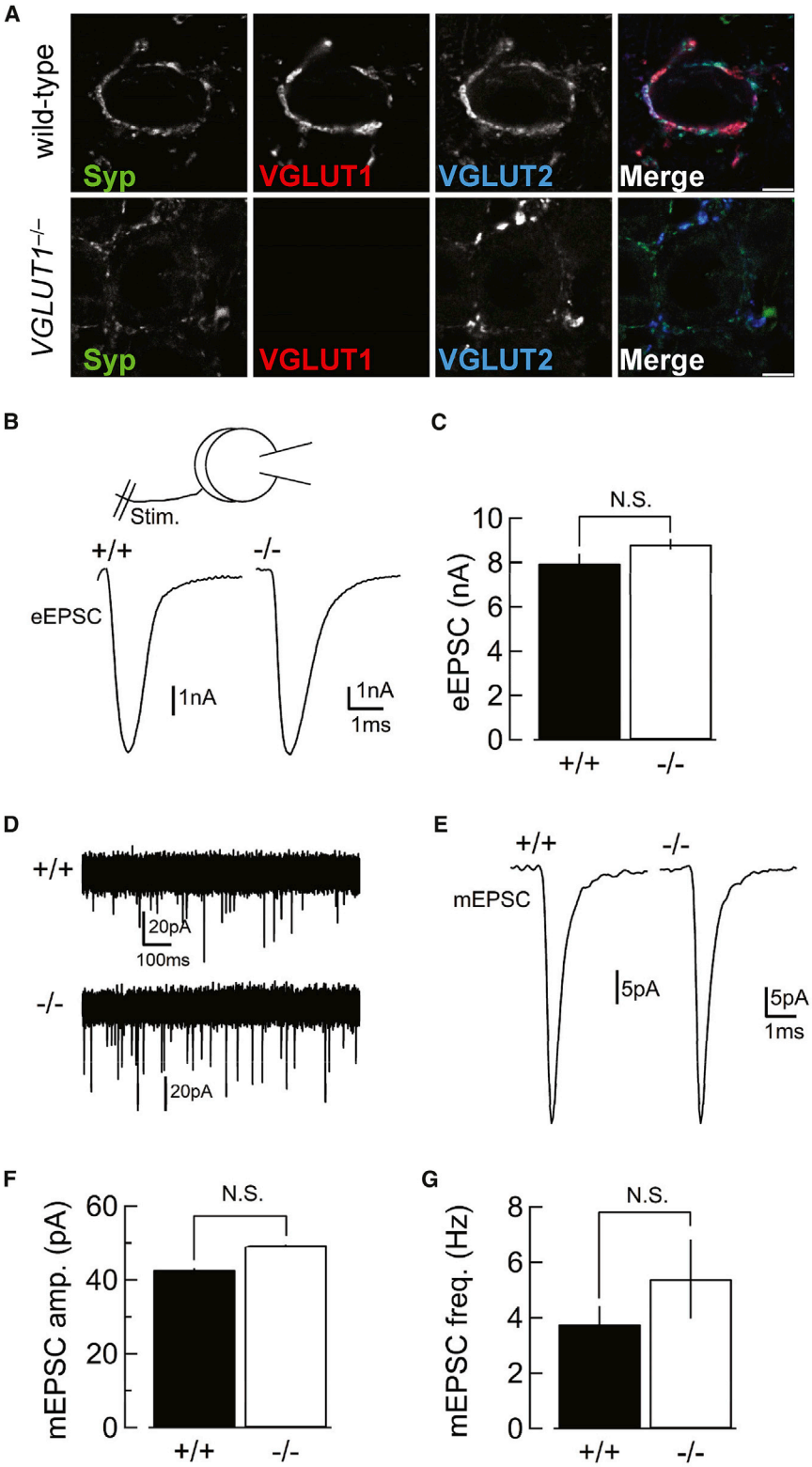


**Figure 1. Normal Evoked and Miniature EPSCs in VGLUT1-Deficient Calyx of Held Synapses**

(A) Immunohistochemistry for VGLUT1 (red), VGLUT2 (blue), and synaptophysin (Syp; green) in wild-type and *VGLUT1*$^{-/-}$ calyx of Held-MNTB synapses. Scale bars indicate 5 μm.

(B) Representative eEPSCs from wild-type (+/+) and *VGLUT1*$^{-/-}$ (−/−) mice.

(C) Mean amplitudes of eEPSCs (no significant difference between +/+ [n = 19] and −/− [n = 24], p = 0.07).

(D) Sample traces of mEPSCs.

(E) Averaged mEPSCs.

(F) Mean amplitudes of mEPSCs (no significant difference between +/+ [n = 11] and −/− [n = 12], p = 0.15).

(G) The mean frequencies of mEPSCs (no significant difference between +/+ [n = 11] and −/− [n = 12], p = 0.16).

Error bars in this and the following figures indicate SEM.

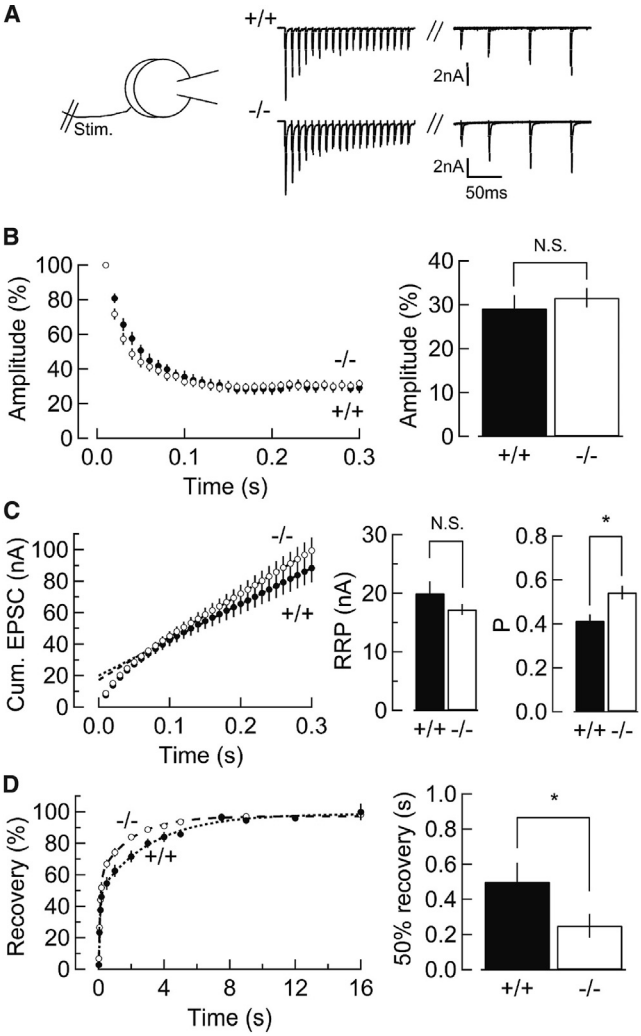


**Figure 2. Slightly Perturbed Short-Term Plasticity and Recovery from Depression in VGLUT-Deficient Calyx of Held Synapses**

(A) Sample traces of EPSCs evoked by a train of 30 stimuli at 100 Hz and by the subsequent test stimuli with various intervals (0.02–16 s).

(B) Normalized EPSCs during a 100 Hz train recorded in +/+ (filled circles, n = 16) and −/− (open circles, n = 23) mice. The bar graph indicates steady-state amplitudes at 0.3 s (no significant difference, p = 0.51).

(C) Cumulative amplitudes of EPSCs during a 100 Hz train. Left bar graph: sizes of readily releasable pool (RRP); 20.0 ± 2.0 nA in +/+ and 17.2 ± 0.9 nA in −/− (not significant, p = 0.17). Right bar graph: release probability (P); 0.41 ± 0.03 in +/+, 0.54 ± 0.03 in −/−.

(D) Recoveries of EPSCs from STD. The recovery of EPSCs was calculated as recovery = $(EPSC_{test} - EPSC_{steady\ state})/(EPSC_{1st} - EPSC_{steady\ state}) \times 100$. The bar graph indicates the half recovery times calculated from double-exponential fittings: 0.50 ± 0.10 s in +/+ (n = 12), 0.25 ± 0.07 s in −/− (n = 19). N.S., no significant difference (p > 0.05); *p < 0.05.

between wild-type and *VGLUT1*$^{-/-}$ (VGLUT2-only) synapses by using standard protocols to assess short-term plasticity, the size of the readily releasable pool (RRP) of SVs, SV release probability, and recovery from synaptic depression.

Short-term depression (STD) was induced by application of a train of 30 stimuli at 100 Hz (0.3 s), and the recovery was monitored by inducing single action potentials (APs) at increasing time intervals after the train (Figure 2A). The relative amplitudes during the steady-state depression phase of the train were not significantly different between the two genotypes (Figure 2B). The RRP size can be estimated from the cumulative plots (Figure 2C) by extrapolating the slope of the cumulative curve at steady state to the values at time point 0, and then the SV release probability can be estimated from the ratio between the initial EPSC amplitude and RRP size. Corresponding analyses showed that *VGLUT1*$^{-/-}$ synapses had the same RRP size as wild-type synapses and exhibited slightly higher release probability than wild-type synapses (Figure 2C). On the other hand, EPSCs recovered significantly more rapidly in *VGLUT1*$^{-/-}$ synapses compared with wild-type controls (Figure 2D). Previous studies using similar experimental protocols demonstrated that RRP replenishment has two components: a fast $Ca^{2+}$-dependent component and a slow $Ca^{2+}$-independent component (Sakaba and Neher, 2001; Wang and Kaczmarek, 1998). To examine whether VGLUT1 loss selectively affects the first component, we performed the same experiments using slice preparations preincubated with a $Ca^{2+}$ chelator, EGTA-AM (Figure S2). Notably, pretreatment with EGTA-AM, in whose presence the slow $Ca^{2+}$-independent component mainly contributes to RRP recovery after STD, abated the differences in recovery kinetics that we observed between wild-type and *VGLUT1*$^{-/-}$ synapses under control conditions (Figure 2D).

## Slower Rate of Glutamate Refilling into SVs in VGLUT1-Deficient Calyx of Held Synapses

The facts that single eEPSCs are normal in *VGLUT1*$^{-/-}$ synapses and that short-term plasticity and synaptic recovery from depression are only very subtly affected offered us the opportunity to reliably monitor the rate of glutamate refilling into SVs in *VGLUT1*$^{-/-}$ synapses. We showed previously that flash photolysis of caged glutamate (MNI-glutamate) after depletion of glutamate from SVs by presynaptic dialysis with a glutamate-free pipette solution causes a recovery of EPSCs that should reflect the time course of glutamate refilling into empty SVs (Figure 3A; Hori and Takahashi, 2012). In typical experiments, EPSCs ran down to <20% of the initial value within 20 min when the afferent fibers were stimulated at 1 Hz while the presynaptic cytoplasm was dialyzed with a glutamate-free solution containing 10 mM caged glutamate. After photolysis, eEPSCs elicited at 1 Hz recovered almost completely in wild-type synapses (Figure S3B; Hori and Takahashi, 2012). In contrast, eEPSCs in *VGLUT1*$^{-/-}$ synapses assessed with the same protocol barely recovered within 15 min after photolysis (Figure S3). In the calyx of Held synapse, a single AP leads to the exocytosis of ~140 of SVs (Neher and Sakaba, 2001; Schneggenburger et al., 1999). Hence, lower stimulation frequencies should report SV refilling kinetics more faithfully, especially if SV refilling rates are very slow and SV reuse occurs before SVs are completely filled with glutamate. We therefore reduced stimulation frequencies from 1 to 0.1 Hz to minimize exocytosis of partially filled SVs, if any, during eEPSC recovery. With this protocol, we observed complete EPSC recovery in *VGLUT1*$^{-/-}$ synapses (Figure 3). The time constants of EPSC recovery were 21.7 ± 5.2 s for wild-type synapses and 81.3 ± 8.8 s for *VGLUT1*$^{-/-}$ synapses

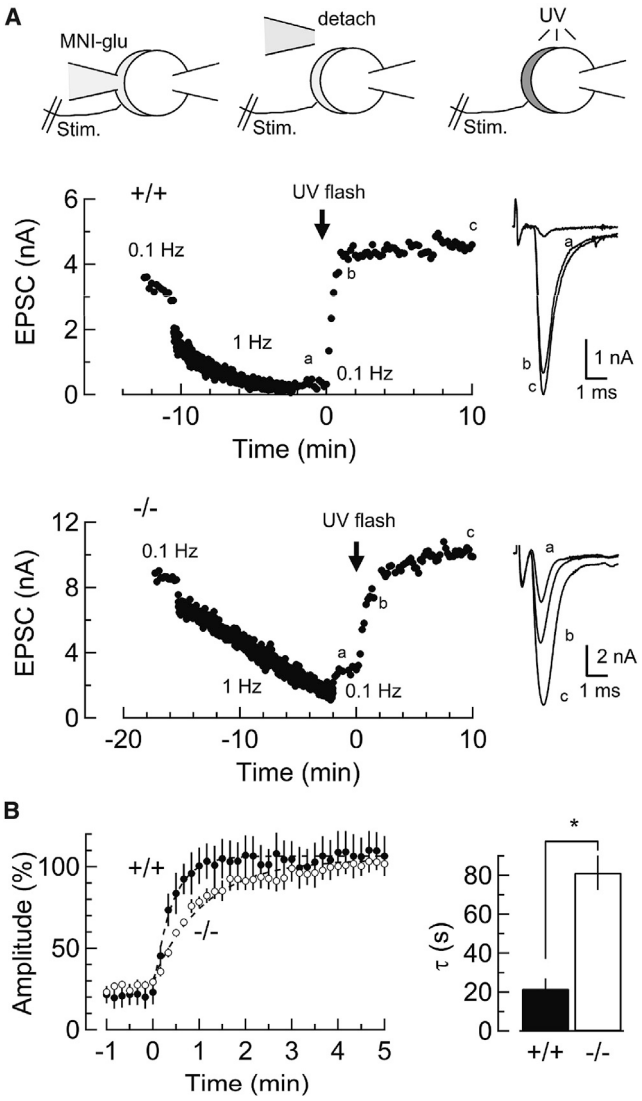


**Figure 3. VGLUT1 Deletion Slows Down Vesicle Refilling with Glutamate**

(A) Upper drawings indicate experimental diagram to monitor glutamate refilling rate (see STAR Methods). Left panels indicate EPSCs during recordings from wild-type (+/+) and *VGLUT1*$^{-/-}$ (−/−) synapses. Right traces were recorded before MNI-glutamate uncaging (a), 50 s after uncaging (b), and 10 min after uncaging (c). Note that stimulation frequencies after uncaging was reduced to 0.1 Hz.

(B) Recoveries of EPSCs after MNI-glutamate uncaging (+/+, filled circles, n = 5; −/−, open circles, n = 4). The right bar graph indicates the time constants of EPSC recoveries fitted by single exponential function. *p < 0.05.

(Figure 3B), indicating that SV refilling in *VGLUT1*$^{-/-}$ synapses is 4 times slower than that in wild-type synapses.

### Slowed-Down SV Refilling Reduces Fidelity of Synaptic Transmission during Sustained High-Frequency Stimulation in VGLUT1-Deficient Calyx of Held Synapses

Given that SV glutamate uptake is considerably slowed down in the absence of VGLUT1, we next tested if the slow SV refilling in *VGLUT1*$^{-/-}$ synapses may become rate limiting for synaptic efficacy under certain conditions, such as sustained high-frequency stimulation. To this end, we first induced STD of EPSCs using a 1,000-train stimulation at 100 Hz (10 s), which resulted in a steady-state EPSC amplitude of 21.8% ± 5.7% of the initial EPSC in wild-type synapses (Figure 4A). In the case of *VGLUT1*$^{-/-}$ synapses, the steady-state EPSC amplitude tended to be smaller (13.4% ± 4.5%) than that in wild-type synapses, although we did not detect statistically significant reductions in the normalized values or the absolute EPSC amplitudes (Figure 4A). We next tested whether the observed trend of reduced steady-state EPSC amplitudes in *VGLUT1*$^{-/-}$ synapses affects synaptic fidelity. To compare the synaptic fidelity between wild-type and *VGLUT1*$^{-/-}$ calyx of Held synapses, we recorded postsynaptic APs with an extracellular patch pipette loosely attached to the MNTB cell body (Eguchi et al., 2012). To evaluate the fidelity of synaptic transmission, we elicited presynaptic APs by injecting depolarizing currents (1 ms) and recorded postsynaptic APs. During presynaptic stimulation at 100 Hz, we never observed failures of postsynaptic APs up to 1,000 stimuli (10 s) in wild-type synapses (Figures 4B and 4C). However, failures of postsynaptic APs were apparent in *VGLUT1*$^{-/-}$ synapses, and the success ratio leveled out at ~60% toward the end of the stimulation train (Figures 4B and 4C). Because APs of postsynaptic cells targeted by *VGLUT1*$^{-/-}$ calyces can follow repetitive current injection with 100 Hz for 10 s (Figure S4A), the reduced synaptic fidelity observed in the *VGLUT1*$^{-/-}$ synapses is very likely of presynaptic origin.

To further confirm that the increased synaptic failure rate can be attributed to the slowed SV refilling rate in *VGLUT1*$^{-/-}$ synapses, we dialyzed the presynaptic terminals of wild-type synapses with pipette solutions containing either a low $Cl^-$ concentration (0.02 mM) or a very high $Cl^-$ concentration (120 mM), both of which slow down the rate of glutamate refilling into SVs, albeit by distinct mechanisms (Eriksen et al., 2016; Hori and Takahashi, 2012; Schenck et al., 2009; Wolosker et al., 1996), and then monitored postsynaptic APs during high-frequency stimulation. Notably, although no synaptic failure was observed in the presence of 30 mM $Cl^-$ in a presynaptic pipette, high-frequency stimulation in the presence of low or high presynaptic $Cl^-$ concentrations resulted in failures of postsynaptic AP generation within several seconds (Figures 4D and S4B). Collectively, these data indicate that the fidelity of synaptic transmission at the calyx of Held synapses is impaired when SV refilling with glutamate is slowed down.

## DISCUSSION

In the present study, we analyzed calyx of Held synapses in brainstem slice preparations derived from *VGLUT1*$^{-/-}$ mice. These synapses normally co-express VGLUT1 and VGLUT2. In contrast, the expression of VGLUT1 and VGLUT2 in most other parts of the central nervous system is complementary and almost mutually exclusive (Fremeau et al., 2001; Fujiyama et al., 2001). Accordingly, previous studies using *VGLUT1*- or *VGLUT2*-knockout mice revealed strongly impaired glutamatergic transmission in brain regions where the predominantly expressed VGLUT isoform was deleted (Fremeau et al., 2004;

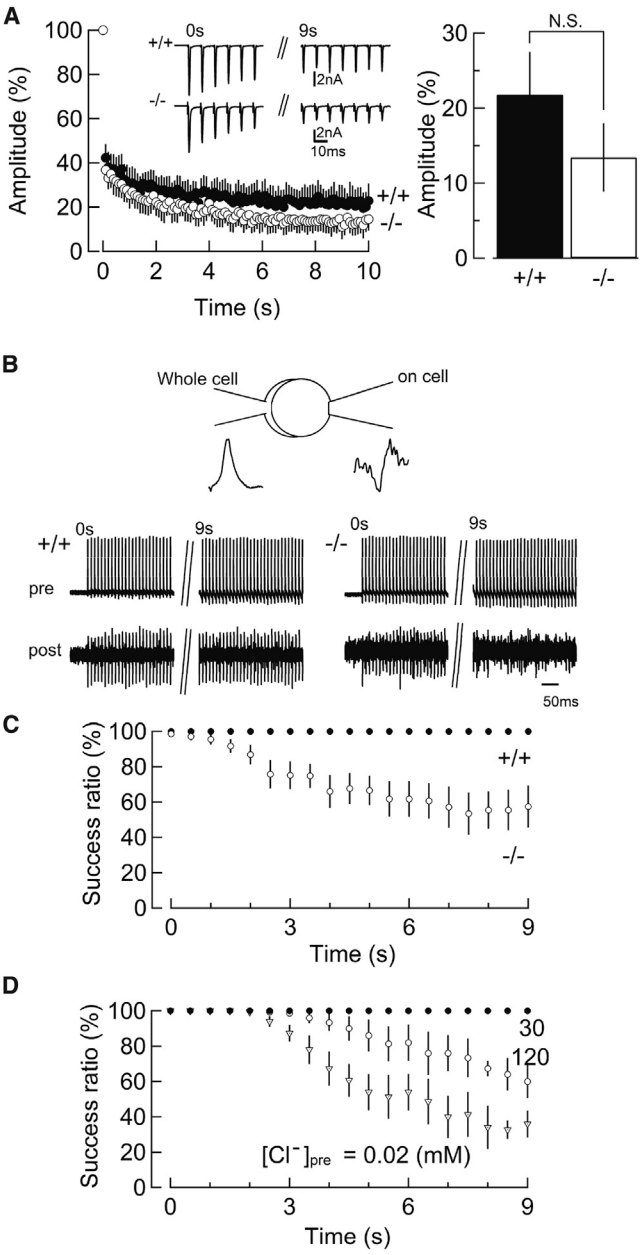


**Figure 4. VGLUT1 Deletion Impairs Synaptic Fidelity during High-Frequency Firing**

(A) Normalized amplitudes of EPSCs evoked by a train of 1,000 stimuli at 100 Hz (+/+, filled circles, n = 4; −/−, open circles, n = 5). Each data point shows the mean amplitudes of the 10 EPSCs. Inset: sample traces of EPSCs at 0 and 9 s, respectively. The bar graph indicates mean EPSC amplitudes of the last 200 EPSCs in a 100 Hz train (no significant difference, p = 0.14).

(B) Top: experimental configuration for measuring input-output relationship of presynaptic and postsynaptic AP firings. Presynaptic APs were evoked by depolarizing current injection through whole-cell patch pipette at 100 Hz. Postsynaptic APs were recorded from an extracellular pipette loosely attached to the somata of a MNTB principal cell. Bottom: sample traces of postsynaptic APs in response to presynaptic APs at 100 Hz. Sample traces derived from different periods at 0 s (left) and 9 s (right) are shown.

(C) The input-output relationship of synaptic transmission. The output/input ratio (success ratio) are plotted as function of time (+/+, filled circles, n = 5; −/−, open circles, n = 7).

(D) The input-output relationship when presynaptic $Cl^-$ concentrations were altered ($[Cl^-]_{pre}$ = 0.02 mM, open triangles, n = 3; $[Cl^-]_{pre}$ = 30 mM, filled circles, n = 5; $[Cl^-]_{pre}$ = 120 mM, open circles, n = 3).

Wojcik et al., 2004), while no changes were observed in synapses that mainly contain the respective other VGLUT isoform (Weston et al., 2011). We found that VGLUT1 loss in calyx of Held synapses has only very minor effects on basal synaptic transmission, likely because of the presence of VGLUT2, but causes a profound reduction of the glutamate refilling rate into SVs. Furthermore, the fidelity of synaptic transmission at *VGLUT1*$^{-/-}$ synapses is impaired during high-frequency stimulation, most likely because of the slowed-down SV refilling rate and the reuse of only partially filled SVs. A recent study on cerebellar inhibitory synapses indicated that GABA refilling into SVs can be rate limiting for inhibitory synaptic transmission because of the intrinsically slow GABA refilling time constant of ~80 s (Yamashita et al., 2018). Our findings now show that this is also the case for glutamatergic transmission when the SV refilling rate is retarded.

The slowed-down SV refilling rate in *VGLUT1*$^{-/-}$ synapses can likely be attributed to two main factors: an overall reduced VGLUT level per SV and/or intrinsic differences between VGLUT1 and VGLUT2 and their SV distribution. With regard to the latter, transport assays did not reveal different glutamate affinities (1–5 mM) and kinetics between VGLUT1 and VGLUT2 (Kaneko and Fujiyama, 2002). Alternatively, the proton-motive force of VGLUT1-containing and VGLUT2-containing SVs at a given synapse could be different, for example, because of differences in the $Cl^-$ dependency of transport, cation/$H^+$ exchange activity, and the copy numbers of V-ATPases (Takamori, 2016), leading to slower glutamate refilling of VGLUT2-containing SVs. However, as VGLUT1 and VGLUT2 seem to be present on the same SVs in calyx of Held synapses, differences in the proton-motive force between VGLUT1-containing and VGLUT2-containing SVs are unlikely to be the cause of the slow SV refilling rate observed in *VGLUT1*$^{-/-}$ synapses. Instead, it is most likely that the reduction of total VGLUT expression in *VGLUT1*$^{-/-}$ synapses causes the slow rate of glutamate refilling. Given that the SV refilling rate is reduced to ~25% in the absence of VGLUT1, the ratio of VGLUT1 and VGLUT2 can be assumed to be 3:1 on average, although immunofluorescence labeling indicated that there are SV clusters that are dominated by one of the two isoforms. Typically, an SV contains ~8–11 VGLUT copies (Takamori et al., 2006). Hence, a given SV in the calyx of Held synapse of *VGLUT1*$^{-/-}$ mice likely contains at least one copy of VGLUT2, which is sufficient to sustain SV filling under conditions of low activity, so that mEPSCs, for instance, are not affected by VGLUT1 loss (Daniels et al., 2006).

*In vitro* glutamate transport assays using isolated SVs and intracellular membranes derived from cell lines expressing VGLUT isoforms indicated that extravesicular (cytoplasmic) $Cl^-$ concentrations profoundly affect VGLUT activity. More recently, luminal $Cl^-$ concentrations were also shown to influence VGLUT activity in proteoliposomes containing recombinant VGLUTs

(Eriksen et al., 2016; Preobraschenski et al., 2014; Schenck et al., 2009). Although the precise mechanisms of the $Cl^-$-dependent regulation of vesicular glutamate uptake have long been debated, a $Cl^-$ conductance of VGLUTs and allosteric binding of $Cl^-$ to VGLUTs are likely involved (Chang et al., 2018). However, the physiological relevance of VGLUT regulation by $Cl^-$ has remained unclear. Whereas in the titration of the cytoplasmic $Cl^-$ concentrations by whole-cell dialysis of calyx of Held synapses revealed a biphasic $Cl^-$ dependency of glutamate uptake into SVs (Hori and Takahashi, 2012), similar manipulations did not alter vesicular glutamate content under resting conditions (Price and Trussell, 2006). Our new results indicate that cytoplasmic $Cl^-$ levels do indeed have a substantial effect on synaptic fidelity under heavy load by modulating the glutamate refilling rate of SVs. Because manipulating luminal $Cl^-$ in the majority of SV populations is not trivial, it remains to be seen whether regulation of VGLUTs by luminal $Cl^-$ is of physiological relevance.

Consistent with previous observations, different VGLUT isoforms appear to determine properties of calyx of Held synapses that are unrelated to transmitter loading into SVs. For instance, VGLUT1-deficient calyx of Held synapses exhibits higher release probability, which is in accord with previous studies on VGLUT-deficient hippocampal neurons or hippocampal slices (Fremeau et al., 2004; Weston et al., 2011). Furthermore, our analyses of recovery from STD revealed that loss of VGLUT1 results in a faster replenishment of the RRP, which is a $Ca^{2+}$-dependent process, indicating that the presence of VGLUT1 proteins on SVs affects the $Ca^{2+}$-dependent mobilization of SVs. Although the molecular mechanisms involved in VGLUT-isoform-specific properties of SV mobilization remain unknown, our results support the notion that distinct VGLUT isoforms differentially affect distinct SV trafficking mechanisms (Guillaud et al., 2017; Voglmaier et al., 2006). It should be noted that in experiments using presynaptic dialysis and subsequent glutamate uncaging, the higher release probability and faster SV replenishment after STD in *VGLUT1*$^{-/-}$ synapses could in principle lead to an underestimation of SV refilling rates. However, the near complete recovery of EPSCs after glutamate uncaging monitored at 0.1 Hz strongly indicates that the facilitated SV recycling in *VGLUT1*$^{-/-}$ synapses should not produce unexpected underestimates of SV refilling rates under these conditions.

We observed synaptic failures within 3 s after the onset of repetitive stimulation in *VGLUT1*$^{-/-}$ synapses, which can be explained only if SV reuse occurs within <3 s in the calyx of Held (i.e., substantially faster than previously assumed) (Neher, 2010). On the other hand, our shorter estimates for the time required for SV reuse are consistent with observations in various preparations, in which pharmacological perturbation of the V-ATPase or dialysis of cytoplasmic neurotransmitters used to block neurotransmitter refilling into SVs caused immediate declines of postsynaptic current (PSC) amplitudes (Ertunc et al., 2007; Hori and Takahashi, 2012; Ikeda and Bekkers, 2009; Yamashita et al., 2018), indicating rapid SV reuse within a few seconds, or even faster during intensive stimulation. This notwithstanding, it is still difficult to imagine that rapidly recycling SVs would contribute to the faster synaptic depression in VGLUT1-decifient synapses, because SV refilling takes much longer ($\tau$ ~20 s at room temperature) (Hori and Takahashi, 2012; this study), so that such reused SVs should be nearly empty at the point of reuse anyway, even in wild-type synapses. To resolve this conundrum, we must assume a mechanism by which SV refilling is substantially accelerated by activity. Indeed, two major cations, $Na^+$ and $Ca^{2+}$, which sharply accumulate in presynaptic terminals during repetitive stimulation, were shown to promote glutamate transport into SVs by serving an optimal driving force (voltage gradient rather than pH gradient) (Huang and Trussell, 2014; Li et al., 2020; Ono et al., 2019). It needs to be seen whether an increase in these cations during high synaptic activity indeed accelerates glutamate refilling into SVs.

Using the calyx of Held synapse as a model system, we show that transmitter refilling into SVs can become rate limiting for synapse function when VGLUT levels are substantially reduced. Given that individual transmitter release sites at calyx of Held synapses are very similar to those in other glutamatergic synapse types (Borst and Soria van Hoeve, 2012), similar scenarios will arise at such synapses. This may be relevant for early developmental phases characterized by low VGLUT1 expression (Wilson et al., 2005; Yamashita et al., 2003) and is of particular importance with regard to the many pathophysiological conditions that entail reductions in VGLUT levels, such as schizophrenia, Alzheimer's disease, and Parkinson's disease (Kashani et al., 2007, 2008; Oni-Orisan et al., 2008).

## STAR★METHODS

Detailed methods are provided in the online version of this paper and include the following:

- KEY RESOURCES TABLE
- RESOURCE AVAILABILITY
  - Lead Contact
  - Materials Availability
  - Data and Code Availability
- EXPERIMENTAL MODEL AND SUBJECT DETAILS
  - Animals
- METHOD DETAILS
  - *VGLUT1*$^{-/-}$ mice
  - Immunohistochemical procedures
  - Slice preparation and solutions
  - Electrophysiological recordings
- QUANTIFICATION AND STATISTICAL ANALYSIS

## SUPPLEMENTAL INFORMATION

Supplemental Information can be found online at https://doi.org/10.1016/j.celrep.2020.108040.

## ACKNOWLEDGMENTS

We are grateful to Drs. Takeshi Kaneko and Reinhard Jahn for antibodies used in this study. This work was supported in part by grants from Japan Society for the Promotion of Science (JSPS) KAKENHI (16H04675, 19H03330), the JSPS Core-to-Core Program, A. Advanced Research Networks grant, and a grant from the Takeda Science Foundation to S.T., a grant from JSPS KAKENHI (18K06493), and a grant from the Naito Foundation to T.H.

## AUTHOR CONTRIBUTIONS

S.T. and T.H. designed experiments and wrote the paper. Y.N., S.A., C.T., and T.H. performed electrophysiological measurements and analyzed the data. T.Y. and M.I. supplied *VGLUT1*$^{-/-}$ animals and performed immunohistochemistry. S.M.W. and N.B. generated *VGLUT1*$^{-/-}$ mice and assisted in finalizing the manuscript.

## DECLARATION OF INTERESTS

The authors declare no competing interests.

Received: January 27, 2020
Revised: July 1, 2020
Accepted: July 24, 2020
Published: August 18, 2020

## REFERENCES

Billups, B. (2005). Colocalization of vesicular glutamate transporters in the rat superior olivary complex. Neurosci. Lett. *382*, 66–70.

Blaesse, P., Ehrhardt, S., Friauf, E., and Nothwang, H.G. (2005). Developmental pattern of three vesicular glutamate transporters in the rat superior olivary complex. Cell Tissue Res. *320*, 33–50.

Borst, J.G., and Soria van Hoeve, J. (2012). The calyx of Held synapse: from model synapse to auditory relay. Annu. Rev. Physiol. *74*, 199–224.

Chang, R., Eriksen, J., and Edwards, R.H. (2018). The dual role of chloride in synaptic vesicle glutamate transport. eLife *7*, e34896.

Chung, C., Barylko, B., Leitz, J., Liu, X., and Kavalali, E.T. (2010). Acute dynamin inhibition dissects synaptic vesicle recycling pathways that drive spontaneous and evoked neurotransmission. J. Neurosci. *30*, 1363–1376.

Daniels, R.W., Collins, C.A., Gelfand, M.V., Dant, J., Brooks, E.S., Krantz, D.E., and DiAntonio, A. (2004). Increased expression of the Drosophila vesicular glutamate transporter leads to excess glutamate release and a compensatory decrease in quantal content. J. Neurosci. *24*, 10466–10474.

Daniels, R.W., Collins, C.A., Chen, K., Gelfand, M.V., Featherstone, D.E., and DiAntonio, A. (2006). A single vesicular glutamate transporter is sufficient to fill a synaptic vesicle. Neuron *49*, 11–16.

Delvendahl, I., Vyleta, N.P., von Gersdorff, H., and Hallermann, S. (2016). Fast, temperature-sensitive and clathrin-independent endocytosis at central synapses. Neuron *90*, 492–498.

Edwards, R.H. (2007). The neurotransmitter cycle and quantal size. Neuron *55*, 835–858.

Egashira, Y., Takase, M., Watanabe, S., Ishida, J., Fukamizu, A., Kaneko, R., Yanagawa, Y., and Takamori, S. (2016). Unique pH dynamics in GABAergic synaptic vesicles illuminates the mechanism and kinetics of GABA loading. Proc. Natl. Acad. Sci. U S A *113*, 10702–10707.

Eguchi, K., Nakanishi, S., Takagi, H., Taoufiq, Z., and Takahashi, T. (2012). Maturation of a PKG-dependent retrograde mechanism for exoendocytic coupling of synaptic vesicles. Neuron *74*, 517–529.

Eriksen, J., Chang, R., McGregor, M., Silm, K., Suzuki, T., and Edwards, R.H. (2016). Protons regulate vesicular glutamate transporters through an allosteric mechanism. Neuron *90*, 768–780.

Ertunc, M., Sara, Y., Chung, C., Atasoy, D., Virmani, T., and Kavalali, E.T. (2007). Fast synaptic vesicle reuse slows the rate of synaptic depression in the CA1 region of hippocampus. J. Neurosci. *27*, 341–354.

Fremeau, R.T., Jr., Troyer, M.D., Pahner, I., Nygaard, G.O., Tran, C.H., Reimer, R.J., Bellocchio, E.E., Fortin, D., Storm-Mathisen, J., and Edwards, R.H. (2001). The expression of vesicular glutamate transporters defines two classes of excitatory synapse. Neuron *31*, 247–260.

Fremeau, R.T., Jr., Burman, J., Qureshi, T., Tran, C.H., Proctor, J., Johnson, J., Zhang, H., Sulzer, D., Copenhagen, D.R., Storm-Mathisen, J., et al. (2002). The identification of vesicular glutamate transporter 3 suggests novel modes of signaling by glutamate. Proc. Natl. Acad. Sci. U S A *99*, 14488–14493.

Fremeau, R.T., Jr., Kam, K., Qureshi, T., Johnson, J., Copenhagen, D.R., Storm-Mathisen, J., Chaudhry, F.A., Nicoll, R.A., and Edwards, R.H. (2004). Vesicular glutamate transporters 1 and 2 target to functionally distinct synaptic release sites. Science *304*, 1815–1819.

Fujiyama, F., Furuta, T., and Kaneko, T. (2001). Immunocytochemical localization of candidates for vesicular glutamate transporters in the rat cerebral cortex. J. Comp. Neurol. *435*, 379–387.

Gras, C., Herzog, E., Bellenchi, G.C., Bernard, V., Ravassard, P., Pohl, M., Gasnier, B., Giros, B., and El Mestikawy, S. (2002). A third vesicular glutamate transporter expressed by cholinergic and serotoninergic neurons. J. Neurosci. *22*, 5442–5451.

Guillaud, L., Dimitrov, D., and Takahashi, T. (2017). Presynaptic morphology and vesicular composition determine vesicle dynamics in mouse central synapses. eLife *6*, e24845.

Herman, M.A., Ackermann, F., Trimbuch, T., and Rosenmund, C. (2014). Vesicular glutamate transporter expression level affects synaptic vesicle release probability at hippocampal synapses in culture. J. Neurosci. *34*, 11781–11791.

Herzog, E., Takamori, S., Jahn, R., Brose, N., and Wojcik, S.M. (2006). Synaptic and vesicular co-localization of the glutamate transporters VGLUT1 and VGLUT2 in the mouse hippocampus. J. Neurochem. *99*, 1011–1018.

Hori, T., and Takahashi, T. (2012). Kinetics of synaptic vesicle refilling with neurotransmitter glutamate. Neuron *76*, 511–517.

Huang, H., and Trussell, L.O. (2014). Presynaptic HCN channels regulate vesicular glutamate transport. Neuron *84*, 340–346.

Ikeda, K., and Bekkers, J.M. (2009). Counting the number of releasable synaptic vesicles in a presynaptic terminal. Proc. Natl. Acad. Sci. U S A *106*, 2945–2950.

Kaneko, T., and Fujiyama, F. (2002). Complementary distribution of vesicular glutamate transporters in the central nervous system. Neurosci. Res. *42*, 243–250.

Kashani, A., Betancur, C., Giros, B., Hirsch, E., and El Mestikawy, S. (2007). Altered expression of vesicular glutamate transporters VGLUT1 and VGLUT2 in Parkinson disease. Neurobiol. Aging *28*, 568–578.

Kashani, A., Lepicard, E., Poirel, O., Videau, C., David, J.P., Fallet-Bianco, C., Simon, A., Delacourte, A., Giros, B., Epelbaum, J., et al. (2008). Loss of VGLUT1 and VGLUT2 in the prefrontal cortex is correlated with cognitive decline in Alzheimer disease. Neurobiol. Aging *29*, 1619–1630.

Li, D., Zhu, Y., and Huang, H. (2020). Spike activity regulates vesicle filling at a glutamatergic synapse. J. Neurosci. *40*, 4972–4980.

Moechars, D., Weston, M.C., Leo, S., Callaerts-Vegh, Z., Goris, I., Daneels, G., Buist, A., Cik, M., van der Spek, P., Kass, S., et al. (2006). Vesicular glutamate transporter VGLUT2 expression levels control quantal size and neuropathic pain. J. Neurosci. *26*, 12055–12066.

Mutterer, J., and Zinck, E. (2013). Quick-and-clean article figures with FigureJ. J. Microsc. *252*, 89–91.

Neher, E. (2010). What is rate-limiting during sustained synaptic activity: vesicle supply or the availability of release sites. Front. Synaptic Neurosci. *2*, 144.

Neher, E., and Sakaba, T. (2001). Combining deconvolution and noise analysis for the estimation of transmitter release rates at the calyx of held. J. Neurosci. *21*, 444–461.

Oni-Orisan, A., Kristiansen, L.V., Haroutunian, V., Meador-Woodruff, J.H., and McCullumsmith, R.E. (2008). Altered vesicular glutamate transporter expression in the anterior cingulate cortex in schizophrenia. Biol. Psychiatry *63*, 766–775.

Ono, Y., Mori, Y., Egashira, Y., Sumiyama, K., and Takamori, S. (2019). Expression of plasma membrane calcium ATPases confers $Ca^{2+}/H^{+}$ exchange in rodent synaptic vesicles. Sci. Rep. *9*, 4289.

Preobraschenski, J., Zander, J.F., Suzuki, T., Ahnert-Hilger, G., and Jahn, R. (2014). Vesicular glutamate transporters use flexible anion and cation binding sites for efficient accumulation of neurotransmitter. Neuron *84*, 1287–1301.

Price, G.D., and Trussell, L.O. (2006). Estimate of the chloride concentration in a central glutamatergic terminal: a gramicidin perforated-patch study on the calyx of Held. J. Neurosci. *26*, 11432–11436.

Sakaba, T., and Neher, E. (2001). Calmodulin mediates rapid recruitment of fast-releasing synaptic vesicles at a calyx-type synapse. Neuron *32*, 1119–1131.

Schenck, S., Wojcik, S.M., Brose, N., and Takamori, S. (2009). A chloride conductance in VGLUT1 underlies maximal glutamate loading into synaptic vesicles. Nat. Neurosci. *12*, 156–162.

Schindelin, J., Arganda-Carreras, I., Frise, E., Kaynig, V., Longair, M., Pietzsch, T., Preibisch, S., Rueden, C., Saalfeld, S., Schmid, B., et al. (2012). Fiji: an open-source platform for biological-image analysis. Nat. Methods *9*, 676–682.

Schneggenburger, R., Meyer, A.C., and Neher, E. (1999). Released fraction and total size of a pool of immediately available transmitter quanta at a calyx synapse. Neuron *23*, 399–409.

Südhof, T.C. (2004). The synaptic vesicle cycle. Annu. Rev. Neurosci. *27*, 509–547.

Takamori, S. (2006). VGLUTs: 'exciting' times for glutamatergic research? Neurosci. Res. *55*, 343–351.

Takamori, S. (2016). Presynaptic molecular determinants of quantal size. Front. Synaptic Neurosci. *8*, 2.

Takamori, S., Rhee, J.S., Rosenmund, C., and Jahn, R. (2001). Identification of differentiation-associated brain-specific phosphate transporter as a second vesicular glutamate transporter (VGLUT2). J. Neurosci. *21*, RC182.

Takamori, S., Holt, M., Stenius, K., Lemke, E.A., Grønborg, M., Riedel, D., Urlaub, H., Schenck, S., Brügger, B., Ringler, P., et al. (2006). Molecular anatomy of a trafficking organelle. Cell *127*, 831–846.

Voglmaier, S.M., Kam, K., Yang, H., Fortin, D.L., Hua, Z., Nicoll, R.A., and Edwards, R.H. (2006). Distinct endocytic pathways control the rate and extent of synaptic vesicle protein recycling. Neuron *51*, 71–84.

Wang, L.Y., and Kaczmarek, L.K. (1998). High-frequency firing helps replenish the readily releasable pool of synaptic vesicles. Nature *394*, 384–388.

Watanabe, S., Rost, B.R., Camacho-Pérez, M., Davis, M.W., Söhl-Kielczynski, B., Rosenmund, C., and Jorgensen, E.M. (2013). Ultrafast endocytosis at mouse hippocampal synapses. Nature *504*, 242–247.

Watanabe, S., Trimbuch, T., Camacho-Pérez, M., Rost, B.R., Brokowski, B., Söhl-Kielczynski, B., Felies, A., Davis, M.W., Rosenmund, C., and Jorgensen, E.M. (2014). Clathrin regenerates synaptic vesicles from endosomes. Nature *515*, 228–233.

Weston, M.C., Nehring, R.B., Wojcik, S.M., and Rosenmund, C. (2011). Interplay between VGLUT isoforms and endophilin A1 regulates neurotransmitter release and short-term plasticity. Neuron *69*, 1147–1159.

Wilson, N.R., Kang, J., Hueske, E.V., Leung, T., Varoqui, H., Murnick, J.G., Erickson, J.D., and Liu, G. (2005). Presynaptic regulation of quantal size by the vesicular glutamate transporter VGLUT1. J. Neurosci. *25*, 6221–6234.

Wojcik, S.M., Rhee, J.S., Herzog, E., Sigler, A., Jahn, R., Takamori, S., Brose, N., and Rosenmund, C. (2004). An essential role for vesicular glutamate transporter 1 (VGLUT1) in postnatal development and control of quantal size. Proc. Natl. Acad. Sci. U S A *101*, 7158–7163.

Wolosker, H., de Souza, D.O., and de Meis, L. (1996). Regulation of glutamate transport into synaptic vesicles by chloride and proton gradient. J. Biol. Chem. *271*, 11726–11731.

Yamashita, T., Ishikawa, T., and Takahashi, T. (2003). Developmental increase in vesicular glutamate content does not cause saturation of AMPA receptors at the calyx of Held synapse. J. Neurosci. *23*, 3633–3638.

Yamashita, T., Hige, T., and Takahashi, T. (2005). Vesicle endocytosis requires dynamin-dependent GTP hydrolysis at a fast CNS synapse. Science *307*, 124–127.

Yamashita, M., Kawaguchi, S.Y., Hori, T., and Takahashi, T. (2018). Vesicular GABA uptake can be rate limiting for recovery of IPSCs from synaptic depression. Cell Rep. *22*, 3134–3141.

## STAR★METHODS

### KEY RESOURCES TABLE

| REAGENT or RESOURCE | SOURCE | IDENTIFIER |
|---|---|---|
| Antibodies | | |
| Rabbit polyclonal anti-VGLUT1 | Takamori et al., 2001 | Shigeo3 |
| Rabbit polyclonal anti-VGLUT3 | Synaptic Systems | Cat# 135-203; RRID: AB_887886 |
| Mouse monoclonal anti-Synaptophysin | A gift from Dr. Reinhard Jahn | Cl7.2 |
| Guinea pig polyclonal anti-VGLUT2 | A gift from Dr. Takeshi Kaneko, Fujiyama et al., 2001 | N/A |
| Alexa 488 goat anti-mouse IgG | Thermo Fisher Scientific | Cat# A11029; RRID: AB_2534088 |
| Alexa 532 goat anti-rabbit IgG | Thermo Fisher Scientific | Cat# A11009; RRID: AB_2534076 |
| Alexa 568 goat anti-guinea pig IgG | Thermo Fisher Scientific | Cat# A11075; RRID: AB_2534119 |
| Chemicals, Peptides, and Recombinant Proteins | | |
| Strychnine hydrochloride | Sigma | Cat# S8753-25G |
| Picrotoxin | Tokyo Chemical Industry | Cat# C0375 |
| MNI-caged-L-glutamate | Cayman Chemical | Cat# 19532 |
| Glutathione (Reduced Form), free acid | Nacalai Tesque | Cat# 17050-14 |
| Qx-314 Cl | Alomone labs | Cat# Q-150 |
| EGTA-AM | AAT Bioquest | Cat# 21005 |
| Experimental Models: Organisms/Strains | | |
| Mouse: C57BL/6NCrSlc | Japan SLC, Inc. | RRID:MGI:5295404 |
| Mouse: *VGLUT1*$^{-/-}$ | Wojcik et al., 2004 | N/A |
| Oligonucleotides | | |
| 3 Primers for genotyping, see Experimental Procedures | This paper | N/A |
| Software and Algorithms | | |
| Fiji (ImageJ) | https://fiji.sc/#cite | RRID: SCR_002285 |
| FigureJ | https://imagej.net/FigureJ | N/A |
| IgorPro 6.2J | WaveMatrics | RRID: SCR_001950 |
| MS Excel 2016 | Microsoft | RRID: SCR_016137 |
| pCLAMP 9 | Molecular Devices | RRID: SCR_011323 |

### RESOURCE AVAILABILITY

#### Lead Contact

Further information and requests for resources and reagents should be directed to and will be fulfilled by the Lead Contact, Dr. Tetsuya Hori (tetsuya.hori@oist.jp).

#### Materials Availability

This study did not generate any unique reagents.

#### Data and Code Availability

This study did not generate any unique datasets or code.

### EXPERIMENTAL MODEL AND SUBJECT DETAILS

#### Animals

Male and female C57BL6N mice and *VGLUT1*$^{-/-}$ mice (postnatal days 16 – 19) were used in accordance with the guideline of the Physiological Society of Japan. *VGLUT1*$^{-/-}$ mice were generated as described previously (Wojcik et al., 2004). Mice were taken care at the animal house, and food and water could be obtained freely. All procedures and animal cares were conducted in

accordance with the guideline of the Physiological Society of Japan, and were approved by Doshisha University Committee for Regulation on the Conduct of Animal Experiments and Related Activities. All efforts were taken to minimize animal numbers.

## METHOD DETAILS

### *VGLUT1*$^{-/-}$ mice

Genotyping of *VGLUT1*$^{-/-}$ mice was performed by PCR with template genomic DNA from mouse tail biopsies according to the original description of the *VGLUT1*$^{-/-}$ strain (Wojcik et al., 2004). Three primers,

#4172: 5′-TTCAGCAGCCCGCGTTCACTATGG-3′,
#4173: 5′-CCCAGCTCAGCCCTCCTCGCACAA-3′, and
#4174: 5′-CGCATCGCCTTCTATCGCCTTCTT-3′,

were used to amplify wild-type allele (280 bp with a pair of #4172 and #4173) and knock-out allele (357 bp with a pair of #4173 and #4174), respectively. *VGLUT1*$^{-/-}$ mice were obtained by crossing *VGLUT1*$^{+/-}$ mice. *VGLUT1*$^{-/-}$ mice are born according to Mendel's law, and survive until 20 – 22 days after birth.

### Immunohistochemical procedures

*VGLUT1*$^{-/-}$ mice or wild-type littermates were killed by decapitation. Brainstems were dissected and fixed in 4% paraformaldehyde in phosphate-buffered saline (PBS) for overnight at 4°C. After soaking with ice-cold PBS, tissues were transferred to 30% sucrose solution (w/v) and incubated overnight at 4°C. The tissues were then embedded in FSC 22 frozen section compound (Leica, Germany), and frozen at –80°C. Transverse cryostat sections (5 μm thickness) were mounted on glass slides, dried at room temperature (RT), and kept at –80°C until use. For immunostaining, slices on glass slides were heated at 80°C for 30 min in sodium citrate buffer (pH 6.0), washed once with PBS, and permeabilized in PBS containing 0.5% Triton X-100 for 15 min at RT. Sections were blocked with Tris-buffered saline (pH 7.4) supplemented with 0.05% Tween20 (TBS-T) and 3% bovine serum albumin for 30 min at RT, and incubated with primary antibodies overnight at 4°C. Triple immunohistochemical labeling for VGLUT1/VGLUT2/synaptophysin (Syp) or for VGLUT2/VGLUT3/Syp were performed by simultaneously labeling with the following primary antibodies: rabbit anti-VGLUT1 polyclonal antibody (1: 1000, Takamori et al., 2001) or rabbit anti-VGLUT3 polyclonal antibody (1:500, Synaptic Systems, Göttingen, Germany), guinea pig anti-VGLUT2 polyclonal antibody (1: 1000, a kind gift from Takeshi Kaneko) and mouse anti-Syp monoclonal antibody (Cl7.2, 1: 200, a kind gift from Reinhard Jahn). After washing with TBS-T three times, Alexa Fluor 532 conjugated anti-rabbit IgG, Alexa Fluor 568 conjugated anti-guinea pig IgG, and Alexa Fluor 488 conjugated anti-mouse IgG (all from Molecular Probes) were simultaneously applied at 1: 200 dilution, and incubated for 1 h at RT. After washing with TBS-T three times, slides were mounted in ProLong Diamond Antifade Mountant reagent (Molecular Probes) and were visualized on a Leica TCS SP8 confocal fluorescence microscope using an HC PL APO CS2 100 × oil-immersion objective lens (NA = 1.40). Image processing was performed using a Fiji software (Schindelin et al., 2012) with a FigureJ plug-in (Mutterer and Zinck, 2013).

Line scan analysis was then performed using image analysis software, Fiji. For quantification, straight lines across punctate structures containing either VGLUT1 or VGLUT2 were manually drawn. Fluorescence intensities over the lines were calculated by plot profile tool in Fiji. The fluorescence intensities were normalized by the highest intensities of individual proteins within the lines. The intensity profiles were created by using an Excel 2016 software (Microsoft).

### Slice preparation and solutions

Transverse auditory brainstem slices (175 μm thick) containing the medial nucleus of the trapezoid body (MNTB) were prepared from wild-type and *VGLUT1*$^{-/-}$ mice (postnatal day 16 – 19) as described previously (Hori and Takahashi, 2012). Before recordings, slices were incubated for 1 h at 36 – 37°C in artificial cerebrospinal fluid (aCSF) containing (in mM): 125 NaCl, 2.5 KCl, 2 $CaCl_2$, 1 $MgCl_2$, 10 glucose, 3 *myo*–inositol, 2 sodium pyruvate, and 0.5 ascorbic acid, 26 $NaHCO_3$, 1.25 $NaH_2PO_4$, (pH 7.3 when bubbled with 95% $O_2$ / 5% $CO_2$). For recordings, an aCSF containing picrotoxin (100 μM) and strychnine hydrochloride (0.5 μM) was routinely used to block inhibitory synaptic currents. For EGTA-AM-pretreatment experiments, slices were incubated in aCSF containing 0.2 mM EGTA-AM (in 0.1% dimethyl sulfoxide (DMSO)) for 30 min and then washed in normal aCSF for, at least, 30 min before recordings as described in a previous report (Wang and Kaczmarek, 1998). Presynaptic pipette solution (A) contained (in mM): 130 potassium methanesulfonate, 12 sodium phosphocreatine, 3 ATP (Mg salt), 0.5 GTP (Na salt), 1 $MgCl_2$, 0.5 EGTA, 40 HEPES (adjusted to pH 7.3–7.4 with KOH). Presynaptic pipette solution (B) contained 130 mM KCl instead of potassium methanesulfonate. Presynaptic pipette solutions containing various $Cl^-$ concentrations (0.02, 30, and 120 mM) were prepared by mixing (A) and (B) solutions in desired proportions. Postsynaptic pipette solution contained (in mM): 130 CsCl, 5 EGTA, 1 $MgCl_2$, 5 QX314, 40 HEPES (adjusted to pH 7.3–7.4 with CsOH). For glutamate uncaging experiments, a presynaptic pipette solution containing MNI–caged–L–glutamate (10 mM, (*S*)–a–amino2,3–dihydro–4–methoxy–7–nitro–d–oxo–1*H*–indole–1–pentanoic acid, Cayman Chemical) with 30 mM $Cl^-$ was freshly prepared and used. To minimize the phototoxic effect of UV flash upon MNI–glutamate uncaging, a portion of potassium methanesulfonate in presynaptic pipette solution was replaced by 20 mM glutathione while $Cl^-$ concentration was fixed at 30 mM.

### Electrophysiological recordings

The calyx of Held presynaptic terminals and postsynaptic principal cells were visually identified with a 60 × water immersion objective lens (Olympus) attached to an upright microscope (Axioskop, Carl Zeiss). For experimental configurations including whole–cell voltage–clamp recordings, the presynaptic and postsynaptic patch pipettes had resistances of 6–9 MΩ and 2–3 MΩ, respectively, and had series resistances of 8–15 MΩ and 4–8 MΩ, respectively. The liquid junction potentials between pipette and external solution were not corrected.

For whole-cell recordings for both evoked excitatory postsynaptic currents (eEPSCs) and miniature EPSCs (Figures 1, 2, 4A, and S2), postsynaptic recordings were made under voltage-clamp modes at the holding potential of –70 mV. eEPSCs were evoked by afferent nerve stimulation using a bipolar platinum electrode placed in the midline of a brainstem slice.

For uncaging experiments, simultaneous pre- and postsynaptic whole–cell recordings were made from a calyceal nerve terminal and postsynaptic principal cell using an Axopatch 700A amplifier (Axon Instruments), while eEPSCs were evoked by afferent nerve stimulation at 1 Hz using a bipolar platinum electrode as above. A glutamate-free solution containing 10 mM MNI-glutamate was loaded into calyces through a presynaptic pipette. We used essentially the same optical settings for glutamate uncaging experiments described in a previous study (Hori and Takahashi, 2012). We estimated the free glutamate concentration achieved under these conditions to be ~2 mM, which is beyond $K_m$ values for VGLUTs.

After EPSC amplitudes became < 20% of the initial EPSC amplitudes, presynaptic patch pipette was detached from a presynaptic terminal (to avoid rapid diffusion of glutamate released upon MNI-glutamate uncaging), and a UV light flash was applied from a mercury lamp light source (100 μW) by opening a shutter (Uniblitz, Vincent Associate) for 1 s under the control of a shutter driver (JML Optical Industries). Initially, EPSCs were evoked at 1 Hz stimulation throughout recordings as reported previously (Hori and Takahashi, 2012). However, stimulation frequencies had to be reduced to 0.1 Hz to observe full recovery of EPSC amplitudes in *VGLUT1*$^{-/-}$ synapses.

For extracellular recordings of postsynaptic action potentials (APs), postsynaptic patch pipettes were filled with aCSF (resistance, 4–8 MΩ) and gently pressed onto a postsynaptic cell to form a loose seal, while presynaptic APs were elicited by a depolarizing pulse (pulse duration, 1ms) injected into calyces in a current-clamp mode.

## QUANTIFICATION AND STATISTICAL ANALYSIS

All electrophysiological recordings were performed at RT (25 – 27°C). All data were low-pass filtered at 10 kHz and digitized at 50 kHz by Digidata 1322A with pClamp 9 software (Axon instruments). Data were then analyzed using IGOR Pro 6.2J (WaveMatrics) and MS Excel 2016 (Microsoft) software. All values were given as mean ± standard error of the mean (s.e.m.), and $p < 0.05$ was taken as a significant difference in Student's paired or unpaired *t*–test. In all figures, error bars indicate mean ± s.e.m.